

## Ch. 16 The Degenerate Remnants of Stars

### p. 557 §16.1 The Discovery of Sirius B

Friedrich Wilhelm Bessel (1784-1846) used stellar parallax to find  $d(\text{Sirius}) = 2.64 \text{ pc}$  (it's the brightest star in the sky due to its proximity).

He found that its path not straight  $\Rightarrow$  companion "Pup" w/  $T \sim 50 \text{ yrs}$  (actually 49.9).

Pup (Sirius B) found by Clark w/ new largest (18") refractor.

$$M_{\text{Sirius A}} = 2.3 M_{\odot}, \quad M_{\text{Sirius B}} = 1.05 M_{\odot} \quad (\text{F16.1+2 p. 558})$$

Hard to observe since  $L_B = 0.03 L_{\odot} \ll L_A = 23.5 L_{\odot}$

Expected to be cool red star, but spectrum measured in 1915  $\Rightarrow$  hot blue-white,  $T = 27,000 \text{ K} \Rightarrow R \sim 5500 \text{ km} \sim R_{\oplus}$ ,  $\bar{\rho} = 3 \times 10^9 \text{ kg/m}^3$ ,  $g = 4.6 \times 10^6 \text{ m/s}^2$ .

This was the 1<sup>st</sup> white dwarf discovered.

### p. 559 §16.2 White Dwarfs

$\sim \frac{1}{4}$  of nearby stars are wd's, but hard to observed due to low  $L$ .

#### Classes of WD Stars

Spectral type D ("dwarf") has several subdivisions.

$\frac{2}{3}$  (incl. Sirius B) are DA (H absorption lines), the rest are DB (He abs.), DC (no lines), DQ (c), DZ (metal lines).

$T = 5000 - 80,000 \text{ K}$  - below ms. (F16.3 p. 561)

#### Central Conditions in White Dwarfs

$$P_c \approx 4 \times 10^{22} \text{ N/m}^2 \approx 1.5 \times 10^6 P_{c,\odot}, \quad T_c \approx \text{several } 10^7 \text{ K}$$

If H were present it would fuse & produce too much  $L$ .

WDs come from stars w/  $M_{\text{ZAMS}} \lesssim 8-9 M_{\odot}$ .

Most have  $M = 0.42 - 0.70 M_{\odot}$  & consist of C, O (some He WDs)

### p. 560 Spectra & Surface Composition

Due to strong gravity, H rises to top & forms thin layer.

### p. 561 Pulsating WDs

WDs w/ surface  $T_e \approx 12,000 \text{ K}$  are in instability strip of HR diagram (Ch. 14), pulsate w/ multiple periods between 100-1000s.

Called ZZ Ceti variables or DAVs (variable DA WDs).

g-mode (gravity wave) oscillations involve "sloshing" of surface layers are mostly horizontal.

there are also hotter DBVs, DOVs, & PMVs (F16.4 p. 562)

Fig. 16.1 White dwarf Sirius B beside Sirius A (Palomar Observatory)

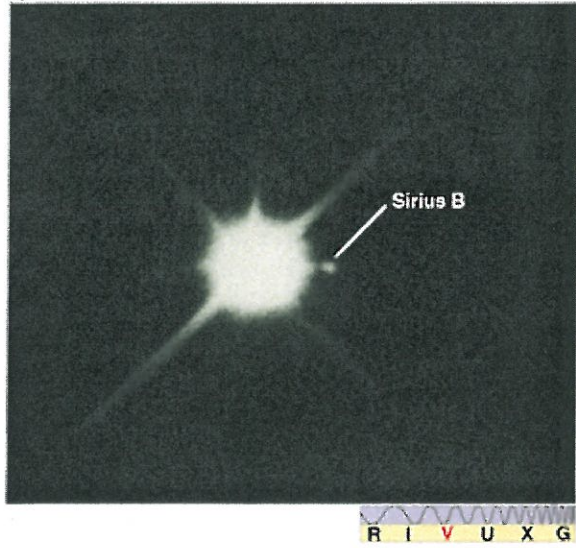


Fig. 16.2 Orbits of Sirius A & B. "x" is center of mass

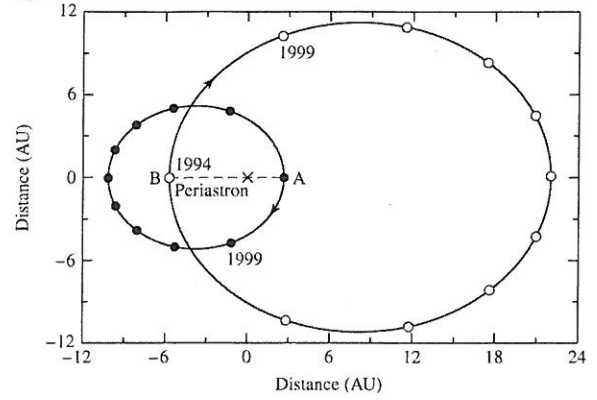


Fig. 16.3 DA white dwarfs on H-R diagram

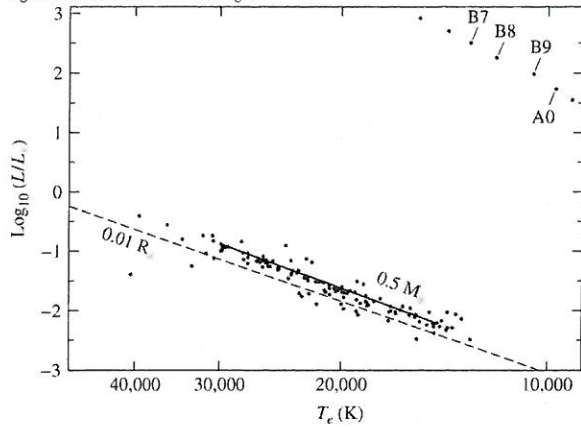


Fig. 16.4 compact pulsators on H-R diagram, from Joshi & Joshi

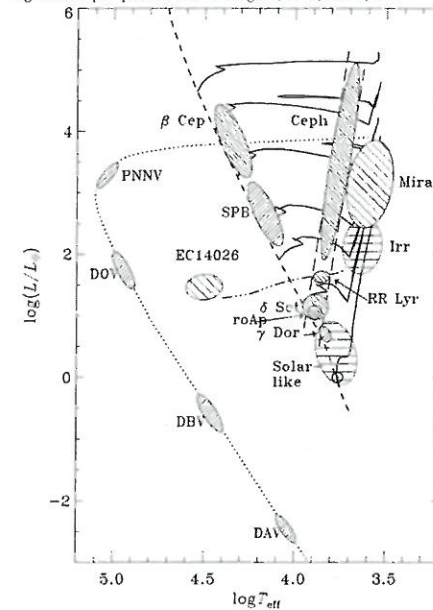


Figure 1: Theoretical HR diagram schematically illustrating locations of known pulsating stars. The dashed line marks the zero-age main sequence (ZAMS) where the solar-like oscillators,  $\gamma$  Doradus,  $\delta$  Scuti and roAp stars are located. The dotted line corresponds to the cooling sequence of white dwarfs, where one finds active planetary-nebula model variable, variable white dwarfs. The parallel log-dashed lines indicate the Cepheid instability strip where RR Lyrae and Cepheids are situated. Adapted from Christensen-Dalsgaard (2000).

p.563 F16.3 The Physics of Degenerate Matter

Normal gas + radiation pressure are insufficient to support a WD.  
Answer was discovered in 1926 - electron degeneracy pressure.

The Pauli Exclusion Principle + Electron Degeneracy

Any particles in any container must be in allowed QM states, specified by 3 quantum #'s (4 if you count spin).

Fermions must obey Pauli Exclusion Principle: no 2 identical fermions in same state.

At normal  $T, P$ , only 1 in  $10^7$  states occupied, so Pauli irrelevant, +  $P \approx$  ideal gas.

But as  $T \downarrow$  or  $\rho \uparrow$ , particles forced into lower energy levels.

$T \rightarrow 0$  K; fermions fill all lowest states, all higher states unoccupied. This is called degeneracy.

Pauli  $\Rightarrow$  most electrons have high  $E$  even at  $T=0 \Rightarrow$  degeneracy pressure.

The Fermi Energy

The highest energy occupied at  $T=0$  is the Fermi energy  $E_F$ .

It is found by equating the # of fermions to the # of states w/  $E < E_F$ .

The result is  $E_F = \frac{\hbar^2}{2m} (3\pi^2 n)^{2/3}$  (F16.5)

$m$  = fermion (electron) mass,  $n = N_e/V$ .

p.565 The Condition for Degeneracy

For complete ionization,  $N_e = \left(\frac{\text{electrons}}{\text{nucleon}}\right) \left(\frac{\text{nucleons}}{\text{volume}}\right) \approx \frac{Z \rho}{A m_H}$

So  $E_F = \frac{\hbar^2}{2m_e} \left[ 3\pi^2 \left(\frac{Z}{A} \frac{\rho}{m_H}\right) \right]^{2/3}$

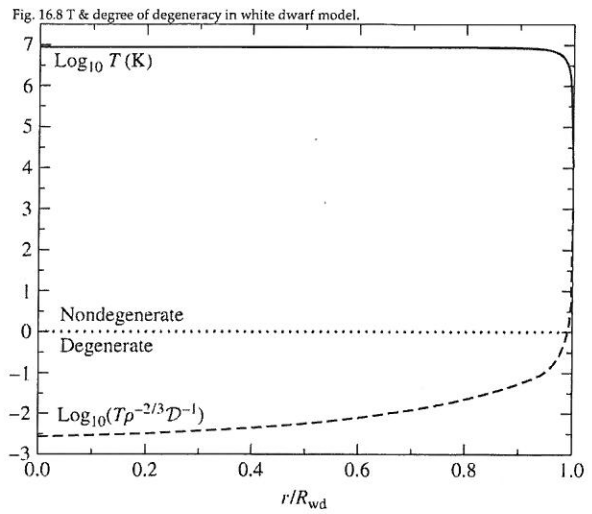
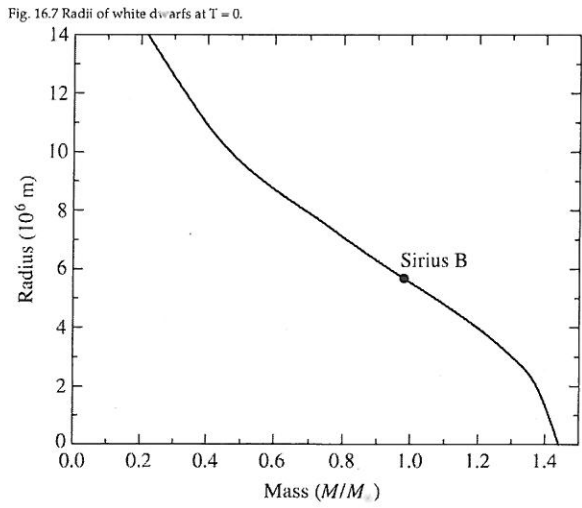
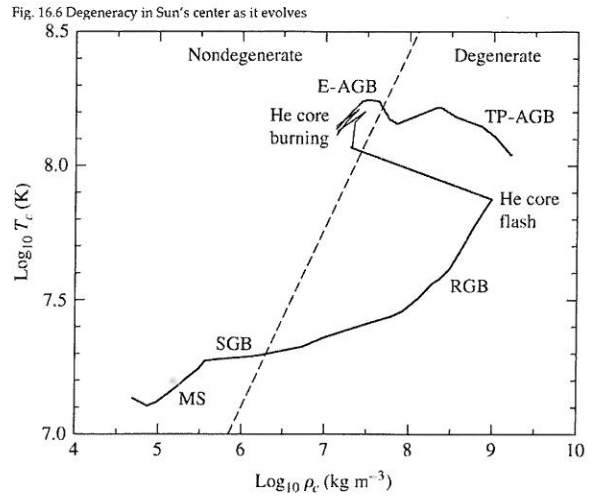
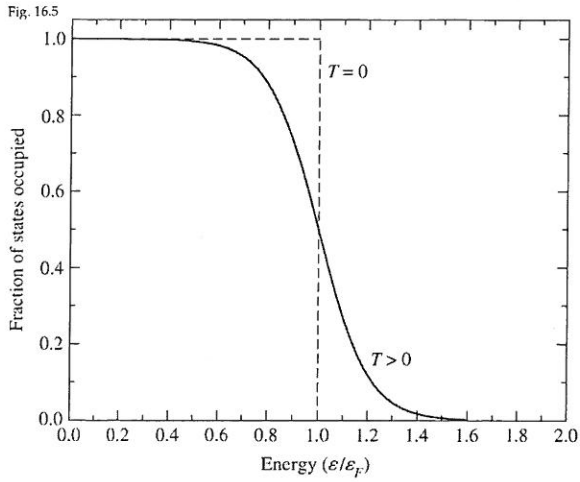
At higher temperatures, some electrons move to higher energy levels. Roughly, e's are degenerate if  $\frac{3}{2} kT < E_F \Rightarrow$

$\frac{I}{\rho^{2/3}} < \mathcal{D} = 1261 \text{ K m}^2 \text{ kg}^{-2/3}$

Ex. 16.3.1 p.566 How important is degeneracy at centers of Sun + Sirius B?

Sun:  $T_c / \rho_c^{2/3} = 1.570 \times 10^7 \text{ K} / [1.527 \times 10^5 \text{ kg m}^{-3}]^{2/3} = 5500 \text{ K m}^2 \text{ kg}^{-2/3} > \mathcal{D} \Rightarrow$  degeneracy weak (F16.6)   
 but more important as it evolved

Sirius B:  $T_c / \rho_c^{2/3} = 7.6 \times 10^7 \text{ K} / [3.0 \times 10^9 \text{ kg m}^{-3}]^{2/3} = 37 \ll 1261 \Rightarrow$  complete degeneracy (it's "cold" at  $7.6 \times 10^7 \text{ K}$ !)



## p. 567 Electron Degeneracy Pressure

Skip derivation

$$P = \frac{(3\pi^2)^{2/3}}{5} \frac{\hbar^2}{m_e} \left[ \left( \frac{Z}{A} \right) \frac{\rho}{m_H} \right]^{5/3}$$

For Sirius B, this is  $1.9 \times 10^{22} \text{ Nm}^{-2}$ , within a factor of 2 of required  $P_c$  (eq. 16.1) needed for support.

Since  $P = K\rho^{5/3}$ , this is a polytrope wr  $n=1.5$ .

## F16.4 The Chandrasekhar Limit (p. 569)

"In 1931, at age 21, Indian physicist Subrahmanyan Chandrasekhar discovered there is a maximum mass for a wd supported by electron degeneracy pressure."

### Mass-Volume Relation

Approximate analysis - equate central pressure estimate 16.1 to electron degeneracy pressure 16.12:

$$\frac{2}{3} \pi G \rho^2 R_{wd}^2 = \frac{(3\pi^2)^{2/3}}{5} \frac{\hbar^2}{m_e} \left[ \left( \frac{Z}{A} \right) \frac{\rho}{m_H} \right]^{5/3}$$

$$\rho = M_{wd} / \frac{4}{3} \pi R_{wd}^3 \Rightarrow R_{wd} \approx \frac{(18\pi)^{2/3}}{10} \frac{\hbar^2}{G m_e M_{wd}^{1/3}} \left[ \left( \frac{Z}{A} \right) \frac{1}{m_H} \right]^{5/3}$$

(actually too small by factor of 2 for  $M = M_\odot$ )

We see  $M_{wd} V_{wd} = \text{constant}$ :  $M \uparrow \Rightarrow V \downarrow$

Actually, as  $M \uparrow$  e's become more relativistic. In the limit where all electrons have  $v=c$ , we find

$$P = \frac{(3\pi^2)^{1/3}}{4} \frac{\hbar c}{m_e} \left[ \left( \frac{Z}{A} \right) \frac{\rho}{m_H} \right]^{4/3}$$

This is a polytrope wr  $\gamma = \frac{4}{3}$ , which is unstable.

Equating this to 16.1 above wr  $\rho = M_{wd} / \frac{4}{3} \pi R_{wd}^3$  gives this estimate for the Chandrasekhar limit (maximum mass):

$$M_{ch} \sim \frac{3\sqrt{2}\pi}{8} \left( \frac{\hbar c}{G} \right)^{3/2} \left[ \left( \frac{Z}{A} \right) \frac{1}{m_H} \right]^2 = 0.44 M_\odot$$

Precise derivation wr  $Z/A = 0.5$  gives  $M_{ch} = 1.44 M_\odot$

No wd has been discovered wr  $M > M_{ch}$ .

(F16.7) is the  $M-R$  relationship for wds.

(Corrections for  $T > 0$ , hard to calculate)

Since  $P$  barely depends on  $T$ , a wd can have He core flash (F13.2) - burning does not expand the core until it becomes non-degenerate.

A low-mass star never burns He, becomes He wd.

### §16.5 The Cooling of White Dwarfs - p. 572 - skip

A  $0.6 M_{\odot}$  wd takes  $\sim 5 \times 10^9$  yr to the point where it crystallizes + becomes a "diamond in the sky".

### §16.6 Neutron Stars p. 578

1932 - Chadwick discovered neutron.

1934 - Baade + Zwicky proposed existence of neutron stars as result of SNe.

#### Neutron degeneracy

Neutrons are fermions, + ns's supported by neutron degeneracy pressure.

Similar to eq. 16.13 for wds,  $R_{ns} \approx \frac{(18\pi)^{2/3}}{10} \frac{\hbar^2}{6M_{ns}^{1/3}} \left(\frac{1}{M_H}\right)^{8/3}$

NS's formed by collapse of degenerate core, so take  $M_{ns} \sim M_{ch} \sim 1.4 M_{\odot}$

$$\Rightarrow R_{ns} \approx 4400 \text{ m (actually 10-15 km)}$$

#### The Density of a NS

$$M, R \Rightarrow \rho \sim 6.65 \times 10^{17} \text{ kg m}^{-3} > \rho_{nuc} \sim 2.3 \times 10^{17} \text{ kg m}^{-3}$$

$$g_{\text{surface}} \sim 1.86 \times 10^{12} \text{ ms}^{-2}$$

Ex. 16.6.1 p. 579 Show that Newtonian mechanics is inadequate.

Escape velocity from surface  $v_{esc} = \sqrt{2GM_{ns}/R_{ns}} = 1.93 \times 10^8 \text{ ms}^{-1} = 0.643c$

Also  $\frac{\text{grav. pot. energy}}{mc^2} = \frac{GM_{ns}m/R_{ns}}{mc^2} = 0.207$  (need GR).

#### The Equation of State

The nature of neutron star matter changes as it is compressed.

At "low" ( $< 10^9 \text{ kg m}^{-3}$ ) density, nucleons are inside Fe nuclei.

$\sim 10^9 \text{ kg m}^{-3}$  the (degenerate) electrons become relativistic + obtain enough energy for  $p^+ + e^- \rightarrow n + \nu_e$  ( $M_n - M_p - m_e = 0.78 \text{ MeV}/c^2$ )

Ex. 16.6.2 p. 580 Estimate  $\rho$  at which  $e^-$  capture begins.

To find minimum velocity for  $p^+ + e^- \rightarrow n + \nu_e$  (ignoring  $E_{\nu}$ ):

$$m_p c^2 + \gamma m_e c^2 = m_n c^2 \Rightarrow \gamma = \frac{m_n - m_p}{m_e} = \frac{1}{\sqrt{1 - v^2/c^2}}$$

$$1 - \frac{v^2}{c^2} = \left(\frac{m_e}{m_n - m_p}\right)^2 \approx 1 - \frac{3\hbar^2}{m_e^2 c^2} \left[\left(\frac{Z}{A}\right) \rho\right]^{2/3} \quad (\text{from 16.10, note that } 3 \text{ is missing on p. 580})$$

$$\rho \approx 4.4 \times 10^9 \text{ kg m}^{-3} \quad (\text{or } 2.3 \times 10^{10} \text{ if you ignore } \nu \text{ as text does})$$

$$\text{Actual value} = 6.2 \times 10^{10} \text{ kg m}^{-3}$$

$\sim 10^{12} \text{ kg m}^{-3} \Rightarrow$  neutronization: lattice of increasingly neutron-rich nuclei:

Fe-56, Ni-62, 64, 66... Kr 111

These n's can't decay back to p's due to  $e^-$  degeneracy.

$\rho \sim 4 \times 10^{14} \text{ kg m}^{-3} \Rightarrow$  neutron drip: 3-component mixture of lattice of nuclei, nonrelativistic degenerate neutrons, relativistic degenerate electrons  
 Neutrons form bosonic pairs  $\Rightarrow$  superfluid (zero viscosity)  
 (no excitations possible).

$\rho > 4 \times 10^{15} \text{ kg m}^{-3}$ : n degeneracy pressure  $>$  e degeneracy pressure

$\rho > \rho_{\text{nuc}} \sim 2 \times 10^{17} \text{ kg m}^{-3}$  nuclei dissolve, fluid of n's, p's, e's. All are superfluid, + p's are superconducting.

n:p:e  $\rightarrow$  8:1:1  
 $\rho > 2 \rho_{\text{nuc}} \sim 4 \times 10^{17} \text{ kg m}^{-3} \Rightarrow$  pions, other particles, quark-gluon plasma?

### p. 581 Neutron Star Models (Table 16.1 p. 582)

Need good e.o.s, + must numerically integrate GR version of stellar structure eqs.

1st quantitative model by J. Robert Oppenheimer + G.M. Volkoff (Berkeley, 1939)

(p. 583) Recent calculation of  $1.4 M_{\odot}$  ns,

Outer crust probably solid lattice + degenerate e's,

Inner crust = nuclear lattice + superfluid n's + degenerate e's,

Interior = superfluid n's + superconducting p's + e's,

Core may be solid w/ exotic particles,

### p. 583 Chandrasekhar Limit for Neutron Stars

Like wd's, ns's obey  $M_{\text{ns}} V_{\text{ns}} = \text{const.} \Rightarrow$   $\exists$  a maximum mass.

Nonrotating  $M_{\text{max}} = 2.2 M_{\odot}$ , rapidly rotating  $\Rightarrow M_{\text{max}} = 2.9 M_{\odot}$

$M > M_{\text{max}} \Rightarrow$  bh

### p. 584 Rapid Rotation + Conservation of Angular Momentum

Using our estimates for  $R_{\text{wd}} + R_{\text{ns}}$ , as the core collapses from wd size

to ns size its radius decreases by the ratio  $\frac{R_{\text{wd}}}{R_{\text{ns}}} \approx \frac{m_{\text{n}}}{m_{\text{e}}} \left(\frac{Z}{A}\right)^{2/3} = 512$

( $Z/A = 26/56$  for Fe)

Moment of inertia  $I = cMR^2$  ( $c = \frac{2}{5}$  for uniform sphere).

$I_i \omega_i = I_f \omega_f \Rightarrow \omega_f = \omega_i (R_i/R_f)^2$

Rotation period  $P_f = P_i (R_f/R_i)^2 \Rightarrow$

$P_{\text{ns}} \approx P_{\text{core}} / 512^2 \approx 3.8 \times 10^{-6} P_{\text{core}}$

$P_{\text{core}}$  probably  $\neq P_{\text{envelope}}$ , so hard to estimate, but use

$P_{\text{core}} = 1350$ s (observed for one wd)  $\Rightarrow P_{\text{ns}} \sim 5 \times 10^{-3}$ s,

Most ns's should be born w/  $P \sim$  several ms.

### p. 585 "Freezing In" Magnetic Field Lines

$\nabla \times \mathbf{B}$  can be shown that B-field lines are "frozen in" to conducting fluid, so

TABLE 16.1 Composition of Neutron Star Material.

| Transition density<br>( $\text{kg m}^{-3}$ ) | Composition  | Degeneracy<br>pressure |
|--|--|------------------------|
| $\approx 1 \times 10^9$                      | iron nuclei,<br>nonrelativistic free electrons   | electron               |
|  | electrons become relativistic  |                        |
| $\approx 1 \times 10^{12}$                   | iron nuclei,<br>relativistic free electrons  | electron               |
|  | neutronization   |                        |
| $\approx 4 \times 10^{14}$                   | neutron-rich nuclei,<br>relativistic free electrons  | electron               |
|  | neutron drip   |                        |
| $\approx 4 \times 10^{15}$                   | neutron-rich nuclei,<br>free neutrons,<br>relativistic free electrons  | electron               |
|  | neutron degeneracy pressure dominates  |                        |
| $\approx 2 \times 10^{17}$                   | neutron-rich nuclei,<br>superfluid free neutrons,<br>relativistic free electrons   | neutron                |
|  | nuclei dissolve  |                        |
| $\approx 4 \times 10^{17}$                   | superfluid free neutrons,<br>superconducting free protons,<br>relativistic free electrons  | neutron                |
|  | pion production  |                        |
|  | superfluid free neutrons,<br>superconducting free protons,<br>relativistic free electrons,<br>other elementary particles (pions, ...?) | neutron                |

Fig. 16.11 A 1.4 M $\odot$  neutron star model

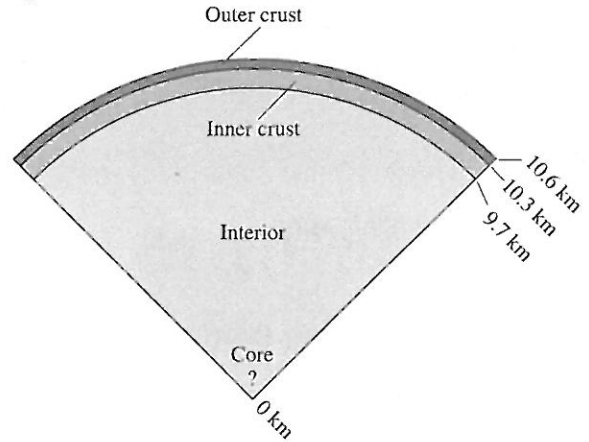


Fig. 16.12

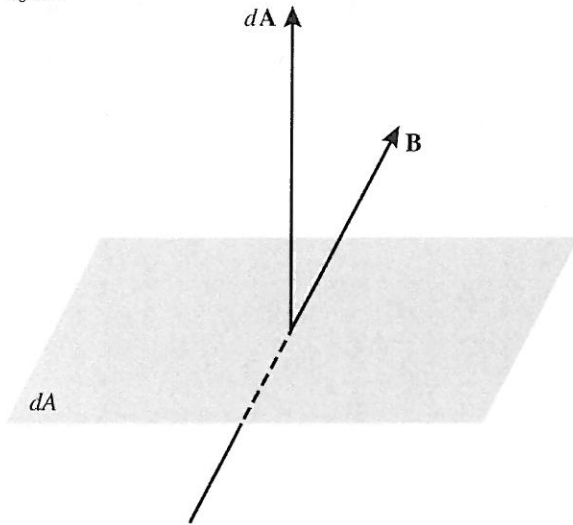


Fig. 16.13 Discovery of the 1st pulsar, PSR 1919+21

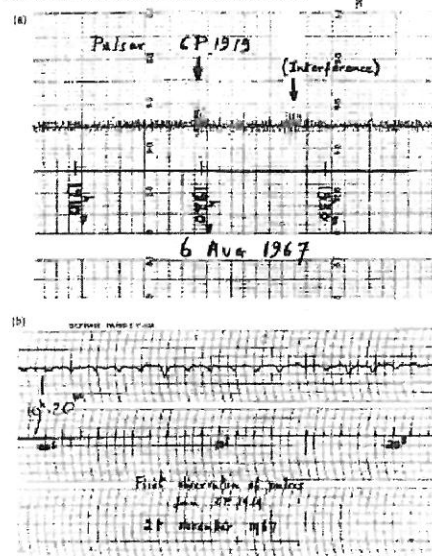


Fig. 1.1. Discovery observations of the first pulsar. (a) The first recording of PSR B1919+21; the signal resembled the radio interference also seen on this chart. (b) First chart recording showing individual pulses as downward deflections of the trace (Hewish et al., 1968).



magnetic flux  $\Phi \equiv \int \vec{B} \cdot d\vec{A}$  is conserved as core collapses.

$$\Rightarrow B_{ns} \approx B_{wd} \left( \frac{R_{wd}}{R_{ns}} \right)^2 \approx 1.3 \times 10^{10} \text{ T if } B_{wd} \approx 5 \times 10^4 \text{ T (extreme value)}$$

More typically  $B_{ns} \sim 10^8 \text{ T} (= 10^{12} \text{ G})$  - + this has been observed.

(The flux-conservation argument is too simplistic, but gives right answer.)

### p. 586 Neutron Star Temperatures

Formed in SN wr  $T \sim 10^{11} \text{ K}$ .

1st deg. - cools by URCA process  $n \rightarrow p^+ + e^- + \bar{\nu}_e$ ,  $p^+ + e^- \rightarrow n + \nu_e$

Energy removed by  $\nu$ 's as quickly as the URCA casino in Brazil removed money from a physicist.

> 1 deg., n's & p's become degenerate so URCA stops, but other  $\nu$ -emitting processes continue for 1000 yr, after which  $\gamma$ 's take over.

$T_{\text{surface}}$  stays at  $\sim 10^6 \text{ K}$  for  $\sim 10^4$  yrs.

$$T = 10^6 \text{ K} \Rightarrow T = 4\pi R^2 \sigma T^4 = 7.13 \times 10^{25} \text{ W} \quad (L_{\odot} = 3.8 \times 10^{26} \text{ W})$$

but unobservable wr satellite, since mainly X-ray:

$$\lambda_{\text{max}} = \frac{(500 \text{ nm})(5800 \text{ K})}{T} = 2.9 \text{ nm} \quad (\text{eg. } 3.19)$$

### p. 586 516.7 Pulsars

Read the story of how PhD student Jocelyn Bell discovered pulsars in 1967 (+ her advisor Anthony Hewish got the Nobel Prize).

She set up 2048 radio antennae to study scintillation of radio waves passing thru solar wind. Saw noise every 400 ft of strip

chart recorder  $\Rightarrow 23 \text{ h } 56 \text{ min} = \text{sidereal period.}$

Closer look  $\Rightarrow$  regular radio pulses wr  $P = 1.337 \text{ s}$ .

Precise natural clock unlikely  $\Rightarrow$  Little Green Men?

Now > 1500 known. (PSR = Pulsating Source of Radiation, or pulsar)

Bell's pulsar = PSR 1919+21:  $\alpha = \text{R.A.} = 19^{\text{h}} 19^{\text{m}}$ ,  $\delta = \text{DEC} = +21^{\circ}$ .

### p. 588 General Characteristics

(F16.14 p 588) Most have  $0.25 \text{ s} < P < 2 \text{ s}$ , but there is a class of millisecond pulsars - the fastest is  $P = 0.00139 \text{ s}$ .

Very well-defined periods: PSR 1937+214 has  $P = 0.00155780644887275 \text{ s}$

Periods increase very slowly:  $\dot{P} \equiv dP/dt \approx 10^{-15}$ ,

Characteristic lifetime  $P/\dot{P} \approx$  several  $10^7$  yr.

### p. 589 Possible Pulsar Models

Hewish, Bell et al. suggested oscillating ns's, but Thomas Gold convincingly argued for rotating ns's.

Fig. 16.14 Distribution of periods for 1533 pulsars

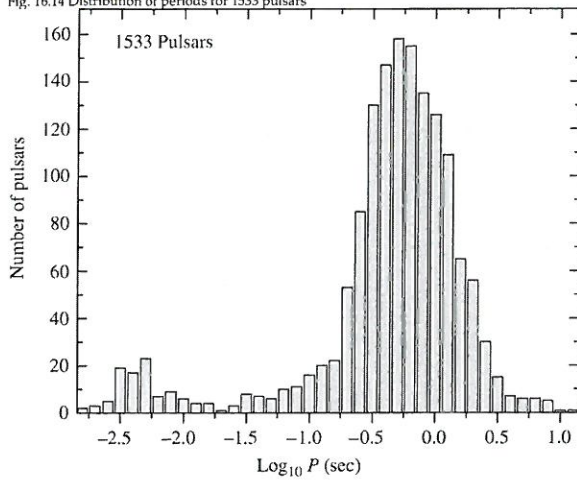


Fig. 16.15 Sequence of images showing flashes at visible wavelengths from Crab pulsar. A foreground star can be seen as the constant point of light above & to left of pulsar.

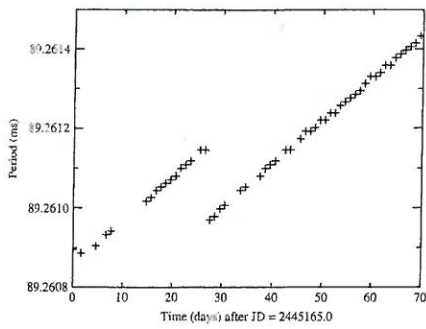
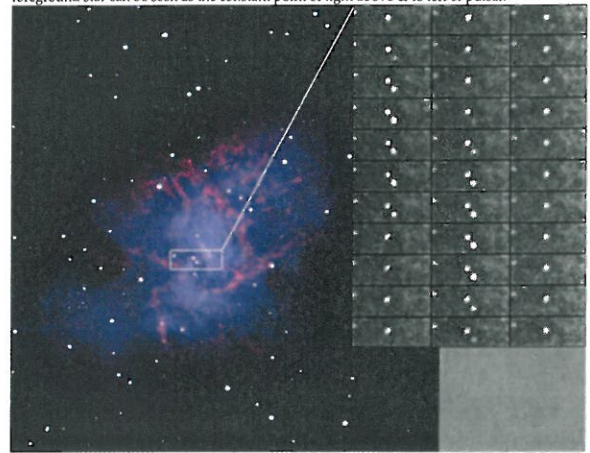
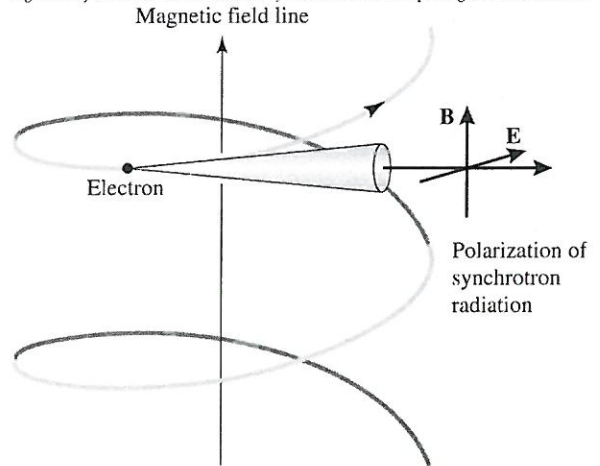


FIGURE 16.16 A glitch in the Vela pulsar. (Figure adapted from McCulloch et al., *Aust. J. Phys.*, 40, 725, 1987.)

Fig. 16.17 Synchrotron radiation emitted by relativistic electron spiraling around B-field line



3 ways to obtain rapid regular pulses in astronomy:

1) Binary stars

For  $P = \bar{P} = 0.79s$ , 2  $1 M_{\odot}$  ns's would have separation  $1.6 \times 10^6 m \Rightarrow$  possible.  
But gravitational radiation  $\Rightarrow$  they would spiral in &  $P \downarrow$ , not  $\uparrow$ .

2) Pulsating stars - but pulsation periods would be too short.

3) Rotating stars

Large  $I$  &  $L \Rightarrow$  pulse period very precise.

Find max rotation rate by equating centripetal acceleration to  $g$ :

$$\omega_{\max}^2 R = GM/R^2 \Rightarrow P_{\min} = 2\pi/\omega_{\max} = 2\pi \sqrt{R^3/GM}$$

Sirius B  $\Rightarrow P_{\min} \hat{=} 7s \Rightarrow$  too long.

$1 M_{\odot}$  ns  $\Rightarrow P_{\min} \hat{=} 5 \times 10^{-4}s \rightarrow$  fine!

p. 590 Pulsars as Rapidly Rotating NSs

Further proof - In 1968 pulsars were found in Vela & Crab SNRs.

(F16.15 p 591 - Crab pulsar) (These young pulsars also produce visible & gamma pulses)

Young pulsars also show glitches, in which  $P$  abruptly decreases

w/  $|\Delta P|/P \approx 10^{-6} - 10^{-8}$  (vortex unpinning) (F16.16 p 591)

Geminga nearest pulsar,  $d = 90 pc$  - has  $\gamma$  & X-ray pulses, but not radio.

p 592 Evidence for a Core-Collapse Supernova Origin

$\geq$  of all stars are in multiple-star systems, but only a few % of pulsars.

Pulsars move faster than most stars, up to  $\sim 1000 km s^{-1}$ .

$\therefore$  Off-center SN that gives the new ns a kick.

Synchrotron & Curvature Radiation

Extrapolate expansion of Crab Nebula backwards, it converges to 90 years after 1054 AD  $\Rightarrow$  it is accelerating.

(F16.17 p 593) Magnetic force on relativistic electron  $\vec{F} = q\vec{v} \times \vec{B}$   
 $\Rightarrow$  helix which follows curved B-field lines.

If circular motion dominates  $\Rightarrow$  synchrotron radiation, linearly polarized in plane of circle.

If curvature of B-field lines dominates  $\Rightarrow$  curvature radiation, linearly polarized in plane of curvature.

Light from some parts of Crab Nebula is 60% linearly polarized.

p 593 Energy Source for Crab's Synchrotron Radiation

To replenish B-field ( $\sim 10^{-4} T$ ) & supply energy to electrons  $\Rightarrow 5 \times 10^{31} W \sim 10^5 L_{\odot}$   
Rate of rotational kinetic energy loss:  $K = \frac{1}{2} I \omega^2 = 2\pi^2 I / P^2$

$$dK/dt = -4\pi^2 I \dot{P} / P^3$$

Ex 16.7.1 p. 594  $I = \frac{2}{5}MR^2$ ,  $R = 10 \text{ km}$ ,  $M = 1.4 M_{\odot}$ ,  $P = 0.0333 \text{ s}$ ,  $\dot{P} = 4.21 \times 10^{-13} \text{ (crab)}$

$\Rightarrow |dK/dt| \approx 5.0 \times 10^{31} \text{ W}$  - yes!

Note: L (pulses) only  $10^{24} \text{ W}$ .

(F16.18 p. 594) too much detail

### p. 595 The Structure of Pulses

Pulses are brief (1-5% of pulse period) (F16.19 p. 595)

Electrons in interstellar space respond more to low frequency waves  $\Rightarrow$

lower frequency radio waves move slower  $\Rightarrow$  dispersion. (F16.20)

The amount of dispersion is a measure of distance to pulsar  $\Rightarrow$  concentrated in galactic plane,  $d = 100$ 's to  $1000$ 's of pc (F16.21 p. 597)

(F16.22 p. 597) Individual pulses very different from average.

Sometimes average pulse shapes switch from 1 mode to another (F16.23)

Sometimes have drifting subpulses (F16.24 p. 598)

30% of pulsars have nulls, in which pulsations disappear for  $\sim 100$  periods.

### p. 596 The Basic Pulsar Model

(F16.25 p. 599) NS w/ mag. dipole axis inclined by  $\theta$  to rotation axis.

Faraday's Law:  $\partial B / \partial t \Rightarrow \vec{E}$

At light  $c$ , cylinder (F16.26 p. 600) these varying B + E fields become em radiation (magnetic dipole radiation)

$$\frac{dE}{dt} = -\frac{32\pi^5 B^2 R^6 \sin^2 \theta}{3\mu_0 c^3 P^4} \quad (B = B_{\text{pole}})$$

If  $dK/dt$  is due to dipole radiation, this =  $-4\pi^2 I \dot{P} / P^3$

$$\Rightarrow B = \frac{1}{2\pi R^3 \sin \theta} \sqrt{\frac{3\mu_0 c^3 I P \dot{P}}{2\pi}}$$

Ex. 16.7.2 p. 599 Crab  $\Rightarrow B = 8.0 \times 10^8 \text{ T}$

$B_{\text{actual}} = 4 \times 10^8 \text{ T}$  ( $\exists$  other torques acting)

### Correlation Between Period Derivatives + Pulsar Classes

There do seem to be distinct classes of pulsar (F16.27 p. 601)

So much useful information!

### p. 600 Toward a Model of Pulsar Emission

Not well understood, but general features...

$\partial B / \partial t \Rightarrow E > 10^{10} \text{ V m}^{-1}$ , pull e's or p's out of surface, create magnetosphere.

Curvature radiation, pair creation cascade...

B is pinned to crust, so  $P = P_{\text{crust}}$ . As ns slows, sometimes quake  $\Rightarrow$   $I \downarrow$  suddenly, or superfluid vortices unpin  $\Rightarrow$  glitch.

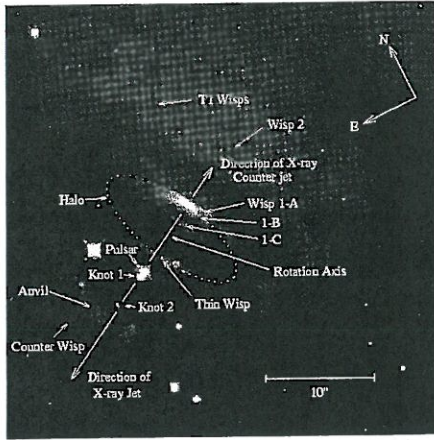


FIGURE 16.18 An HST image of the immediate surroundings of the Crab pulsar. (Hester et al., *Ap. J.*, 448, 240, 1995.)

Fig. 16.19 Pulses from PSR 0329+54 w/ period 0.714 s

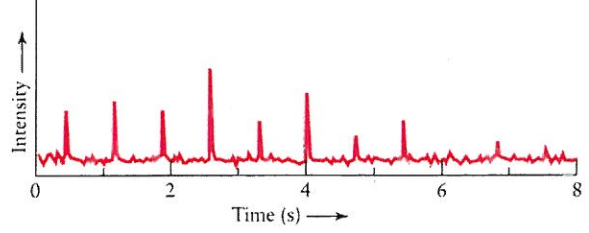


Fig. 16.20

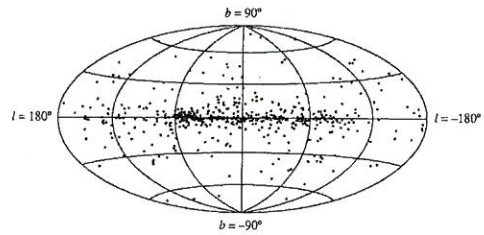
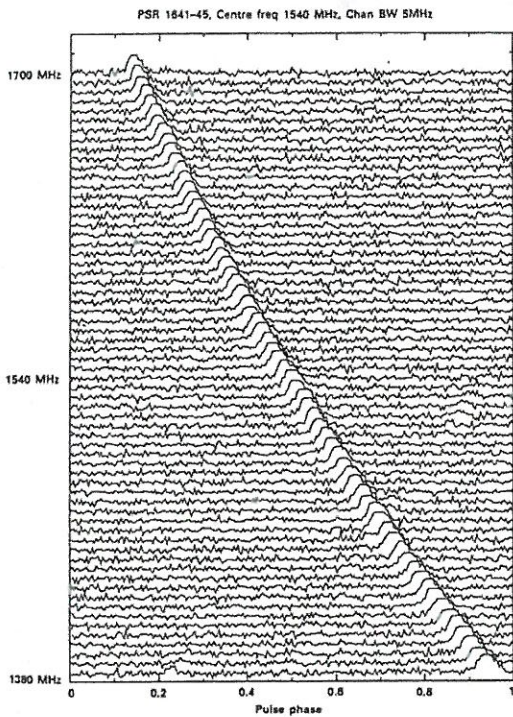


FIGURE 16.21 Distribution of 558 pulsars in galactic coordinates, with the center of the Milky Way in the middle. The clump of pulsars at  $l = 60^\circ$  is a selection effect due to the fixed orientation of the Arecibo radio telescope. (Figure from Taylor, Manchester, and Lyne, *Ap. J. Suppl.*, 88, 529, 1993.)

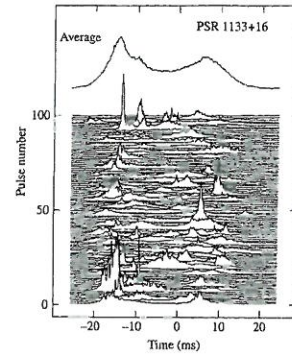


FIGURE 16.22 The average of 500 pulses (top) and a series of 100 consecutive pulses (below) for PSR 1133+16. (Figure adapted from Cordes, *Space Sci. Review*, 24, 567, 1979.)

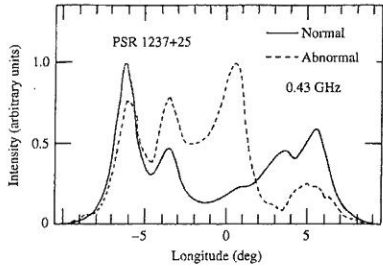


FIGURE 16.23 Changes in the integrated pulse profile of PSR 1237+25 due to mode. This pulsar displays five distinct subpulses. (Figure adapted from Bartel et al., *Ap. J.*, 258, 7)

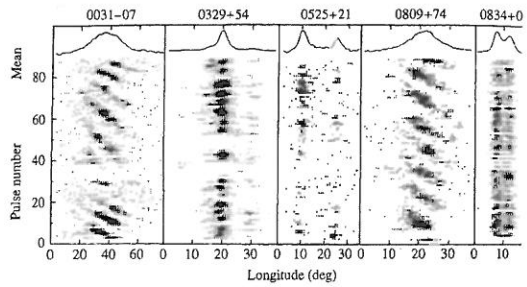


FIGURE 16.24 Drifting subpulses for two pulsars; note that PSR 0031-07 also nulls. (Fi Taylor et al., *Ap. J.*, 195, 513, 1975.)

Fig. 16.25 A basic pulsar model.

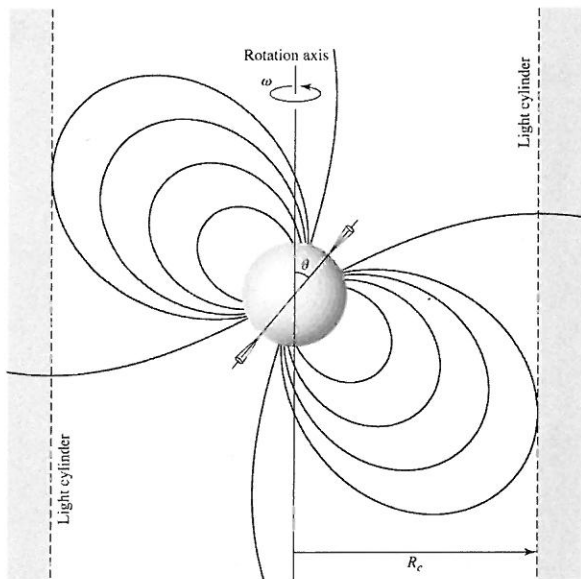
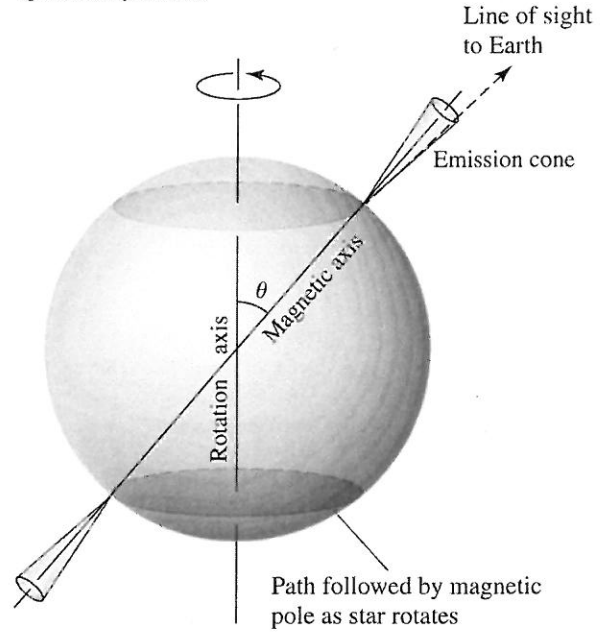
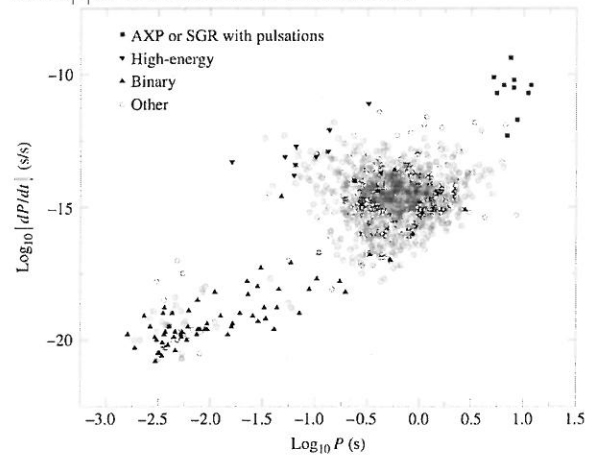


Fig. 16.26 Light cylinder around rotating neutron star

Fig. 16.27  $\dot{P}$  vs  $P$  for all pulsars for which  $\dot{P}$  has been determined.



## p. 602 Magnetars + Soft Gamma Repeaters

Magnetar = ns wr  $B \sim 10^{11} T$ ,  $P = 5-8s$ , may be source of SGRs (soft gamma-ray repeaters).

Correlated wr young ( $\sim 10^4$  yr) SNRs.

Emission mechanism - B-field stresses cause crust to crack, resulting in huge release of energy.

## Ch. 17 General Relativity + Black Holes

### §17.1 The General Theory of Relativity p. 609

Newtonian gravity  $F = G \frac{Mm}{r^2}$  worked fine, except for an inconsistency in the perihelion shift of Mercury (Fig 17.1)

Perihelion shifts by  $574''$ /century,  $43''$  more than predicted by Newtonian grav.

GR is a more accurate theory of gravity + predicts it correctly.

#### The Curvature of Spacetime

Special Relativity (SR) is special in dealing only w/ constant velocity.

GR was developed by Einstein in 1907-15

GR is a geometric theory. (Fig 17.2 p. 611) Mass curves spacetime + curved spacetime tells mass how to move.

Gravity also bends the path of light (Fig. 17.3 p. 611)

Spacetime is curved thru 4<sup>th</sup> spatial dimension. Light takes shortest path in this curved spacetime (Fig 17.4 p. 612)

Dotted line ACB in Fig. 3 + 4 looks shorter, but is actually longer.

Also, time runs slower at point C - both effects contribute equally to making the solid line the shorter (time) path.

GR has been experimentally verified.

AE himself did the calculations of the perihelion shift of Mercury.

"For a few days, I was beside myself with joyous excitement"

Light-bending was measured by Arthur Eddington in the solar eclipse of 1919. ( $1.75''$ ) (Fig. 17.5 p. 613)

### p. 613 The Principle of Equivalence

There are 2 kinds of mass - inertial mass  $F = M_i a$  + gravitational mass  $F_g = G \frac{M M_g}{r^2}$ .

It is an experimental fact that  $M_i = M_g$  to 1 part in  $10^{12}$ , but this is inexplicable in Newtonian mechanics.